Antimicrobial Agents and Chemotherapy

A Combined Pharmacodynamic Quantitative and Qualitative Model Reveals the Potent Activity of Daptomycin and Delafloxacin against Staphylococcus aureus Biofilms

Julia Bauer, Wafi Siala, Paul M. Tulkens and Françoise Van Bambeke

Antimicrob. Agents Chemother. **2013, 57(6):2726. DOI: 10.1128/AAC.00181-13.**
Published Ahead of Print 9 April 2013.

AAC Journals.ASM.org

A Combined Pharmacodynamic Quantitative and Qualitative Model Reveals the Potent Activity of Daptomycin and Delafloxacin against *Staphylococcus aureus* Biofilms

Julia Bauer,* Wafi Siala, Paul M. Tulkens, Françoise Van Bambeke

Pharmacologie cellulaire et moléculaire, Louvain Drug Research Institute, Université catholique de Louvain, Brussels, Belgium

Biofilms are associated with persistence of *Staphylococcus aureus* infections and therapeutic failures. Our aim was to set up a pharmacodynamic model comparing antibiotic activities against biofilms and examining in parallel their effects on viability and biofilm mass. Biofilms of *S. aureus* ATCC 25923 (methicillin-sensitive *S. aureus* [MSSA]) or ATCC 33591 (methicillin-resistant *S. aureus* [MRSA]) were obtained by culture in 96-well plates for 6 h/24 h. Antibiotic activities were assessed after 24/48 h of exposure to concentrations ranging from 0.5 to 512 times the MIC. Biofilm mass and bacterial viability were quantified using crystal violet and the redox indicator resazurin. Biofilms stained with Live/Dead probes were observed by using confocal microscopy. Concentration-effect curves fitted sigmoidal regressions, with a 50% reduction toward both matrix and viability obtained at sub-MIC or low multiples of MICs against young biofilms for all antibiotics tested. Against mature biofilms, maximal efficacies and potencies were reduced, with none of the antibiotics being able to completely destroy the matrix. Delafloxacin and daptomycin were the most potent, reducing viability by more than 50% at clinically achievable concentrations against both strains, as well as reducing biofilm depth, as observed in confocal microscopy. Rifampin, tigecycline, and moxifloxacin were effective against mature MRSA biofilms, while oxacillin demonstrated activity against MSSA. Fusidic acid, vancomycin, and linezolid were less potent overall. Antibiotic activity depends on biofilm maturity and bacterial strain. The pharmacodynamic model developed allows ranking of antibiotics with respect to efficacy and potency at clinically achievable concentrations and highlights the potential utility of daptomycin and delafloxacin for the treatment of biofilm-related infections.

Staphylococcus aureus is a major human pathogen, implicated in both hospital- and community-acquired infections. In addition to the increase in antibiotic resistance that often limits therapeutic options, pathogenic bacteria can adapt and survive in specific microenvironments that are also associated with therapeutic failure and recurrence or persistence of infection. Among them, biofilms play a significant role in persistent infections formed on the surface of implanted medical devices and in deep tissues (1–3). Biofilms are complex aggregates of bacteria encased in an extracellular matrix made of polymeric substances like DNA, polysaccharides, teichoic acids, and proteins (4). Biofilms protect bacteria from host defense and antibiotics, allowing them to remain dormant for long periods in the host, and represent a reservoir for resistance development and for bacterial dissemination within the body. Biofilm formation and growth are finely regulated and are accompanied by metabolic changes that could also affect bacterial response to antibiotics (5).

Antibiotic activity against staphylococcal biofilms has been studied in a large variety of *in vitro* or animal models in an attempt to identify the best therapeutic options. These studies typically evaluate a limited set of drugs in parallel (6–15) and mainly focus on their effect on viability (6–17). Some reports have measured effects on the biofilm matrix, but these are limited to specific antibiotic concentrations (18, 19). Thus, only few studies evaluate antibiotics on a pharmacodynamic basis and compare them in a single model in order to provide useful information regarding their respective interest for treating biofilm-related infections. In this work, we have established a model that allows the quantification of antibiotic potency and efficacy for both bacterial viability and matrix within staphylococcal biofilms, while at the same time visualizing these effects throughout the 3-dimensional structure of the biofilm. This approach has generated coherent and complementary pieces of information that may help rationalize antibiotic selection for biofilm-associated infections.

MATERIALS AND METHODS

Bacterial strains and biofilm culture conditions. *S. aureus* ATCC 25923 (methicillin-sensitive *S. aureus* [MSSA]) and ATCC 33591 (methicillin-resistant *S. aureus* [MRSA]) were used. Biofilms were grown in 96-well plates (European catalog number 734-2327; VWR, Radnor, PA;) with a total volume of 200 μl of medium per well and a starting inoculum approximately equal to 10^7 CFU/ml (optical density at 620 nm [OD_{620}] of 0.005). Biofilm production is described as highly dependent on the temperature of the culture medium (20, 21). Preliminary experiments showed that a strong biofilm was obtained at 30°C in Bacto tryptic soy broth (TSB; Becton, Dickinson, Franklin Lakes, NJ) supplemented with 0.25% glucose and 0.5% NaCl for the two strains investigated here. Growth was allowed for 6 h or 24 h to obtain young and mature biofilms, respectively.

Received 27 January 2013 Returned for modification 28 February 2013
Accepted 29 March 2013
Published ahead of print 9 April 2013
Address correspondence to Françoise Van Bambeke, francoise.vanbambeke@uclouvain.be.
* Present address: Julia Bauer, AppliChem GmbH, Darmstadt, Germany.
J.B. and W.S. contributed equally to the study and share first authorship.
Supplemental material for this article may be found at http://dx.doi.org/10.1128/AAC.00181-13.

doi:10.1128/AAC.00181-13

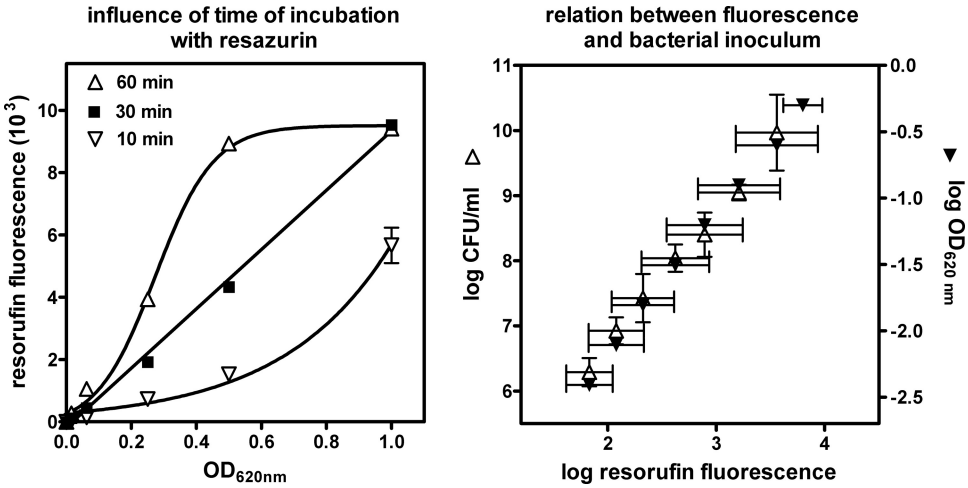

FIG 1 Setting up the resazurin assay with MSSA ATCC 25923. (Left) Resorufin fluorescence signal recorded after 10, 30, or 60 min of incubation of planktonic bacteria at increasing inocula (optical densities) with 10 μg/ml resazurin. (Right) Correlation between resorufin fluorescence signal after 30 min of incubation of planktonic cultures with 10 μg/ml resazurin and bacterial inoculum as evaluated by the number of CFU or the optical density of the suspension. Data are means ± standard deviations [SD] of 2 independent experiments performed in triplicates.

Assessment of biofilm production and of bacterial viability within the biofilm. Biofilm production was evaluated by measuring the absorbance of crystal violet, a cationic dye which stains nonspecifically negatively charged biofilm constituents based on ionic interactions (22). Viability was determined using the blue-colored phenoxazin dye resazurin, which is reduced by viable bacteria to the pink, fluorescent compound resorufin (23, 24). In brief, at the end of the incubation period, the medium was removed and wells were washed twice with 250 μl of phosphate-buffered saline (PBS). For the crystal violet assay, biofilms were fixed by heat at 60°C for about 1 h and stained by 15 min of incubation at room temperature with 150 μl of a 2.3% crystal violet solution prepared in 20% ethanol (Sigma-Aldrich, St. Louis, MO). We checked in preliminary experiments that this volume of crystal violet solution was sufficient to fully cover the biofilm. After elimination of the excess of crystal violet under running water, the dye fixed to the biofilm was resolubilized by the addition of 200 μl of 33% glacial acetic acid and incubation at room temperature for 1 h without shaking. Crystal violet absorbance was measured at 570 nm using a microplate spectrophotometer (VersAmax tunable microplate reader; Molecular Devices, Sunnyvale, CA). For the resazurin assay, biofilms were incubated with 10 μg/ml resazurin (Sigma-Aldrich) in TSB for 30 min at room temperature in the dark. Resorufin fluorescence was measured at a wavelength of 590 nm, with an excitation wavelength of 550 nm (SPECTRAmax spectrofluorometer; Molecular Devices).

Antibiotic susceptibility testing and activity against bacteria growing in biofilms. MICs were determined by microdilution according to CLSI recommendations (25). Antibiotic activity was also evaluated against 6-h and 24-h biofilms. When the desired maturity was reached, the biofilm culture medium was removed and immediately replaced by the same medium (control) or medium containing antibiotics at increasing concentrations (0.5- to 512-fold the MICs in broth). Biofilms were reincubated for 24 h (6-h biofilms) or 48 h (24-h biofilms) at 30°C, and then crystal violet absorbance or resorufin fluorescence was measured as described above. To correct for growth of the biofilm during incubation, all data are expressed as percentages of the results for the matching control.

Confocal microscopy. The BacLight Live/Dead bacterial viability kit (L-7007; Molecular Probes, Eugene, OR) was used to stain bacteria in biofilms grown on glass coverslips. The kit contains (i) Syto9, a membrane-permeable fluorophore staining both living and dead cells in green by intercalation in their DNA, and (ii) propidium iodide, which only enters damaged cells, causing an attenuation of the Syto9 signal in dead cells only and making them appear red when a dual-emission filter is used (26, 27). The stain was prepared by dilution of 4 μl of component A (1.67 mM Syto9 plus 1.67 mM propidium iodide) and 6 μl of component B (1.67 mM syto9 plus 18.3 mM propidium iodide) into 1 ml of distilled water. Biofilms were washed with distilled water, and then coverslips were transferred into a fresh well and incubated for 30 min at room temperature in the dark with 200 μl of staining solution and 100 μl of distilled water, washed again, and directly observed with a 63× lens objective by confocal laser scanning microscopy (CSLM) in a Cell Observer SD microscope (Zeiss) combined with a CSU-X1 spinning disk (Yokogawa) and controlled by AxioVision software (AxioVs40, version 4.8.2.0), with excitation at 488 nm and emission detected using a dual-band emission filter (500 to 550 nm/598 to 660 nm). All settings (camera exposure time and CSU disk speed) were determined in a preliminary experiment and maintained constant throughout. Antibiotic effects were evaluated by determining the fluorescence ratio at 500 nm and 620 nm (after subtraction of background signals) in different focus planes within the depth of the biofilm (z-stack of 1 μm). This ratio being proportional to the number of viable/nonviable cells (BacLight Live/Dead bacterial viability kit; Molecular Probes, Inc.), viability was then calculated from a titration curve established as described in Figure S1 in the supplemental material.

Data analyses and statistical analyses. Curve-fitting analyses were made using GraphPad Prism version 4.03 (GraphPad Software, San Diego, CA, USA). Data were used to fit mono- or biphasic sigmoidal regressions. This allowed us to calculate maximal efficacy (E_{max}; maximal reduction in biofilm mass production or in viable bacteria extrapolated for an infinitely large concentration) and relative potencies (concentrations allowing 25, 50, or 75% reduction of the parameter investigated [C_{25}, C_{50}, or C_{75}, respectively]). Statistical analyses were made with GraphPad Instat, version 3.06 (GraphPad Software).

Source of antibiotics. The following antibiotics were obtained as microbiological standards from their respective manufacturers: daptomycin from Novartis Pharma AG (Basel, Switzerland), moxifloxacin from Bayer HealthCare (Leverkusen, Germany), fusidic acid from Cempra Pharmaceuticals (Chapel Hill, NC), and delafloxacin from Rib-X Pharmaceuticals (New Haven, CT). Additional antibiotics were obtained as the brand-name commercial products available for human use in Belgium (vancomycin as Vancocin [GlaxoSmithKline s.a./n.v., Genval, Belgium], rifampin as Rifadine [Merrell Dow Pharmaceuticals, Inc., Strasbourg, France], and linezolid as Zyvoxid [Pfizer s.a./n.v., Brussels, Belgium]).

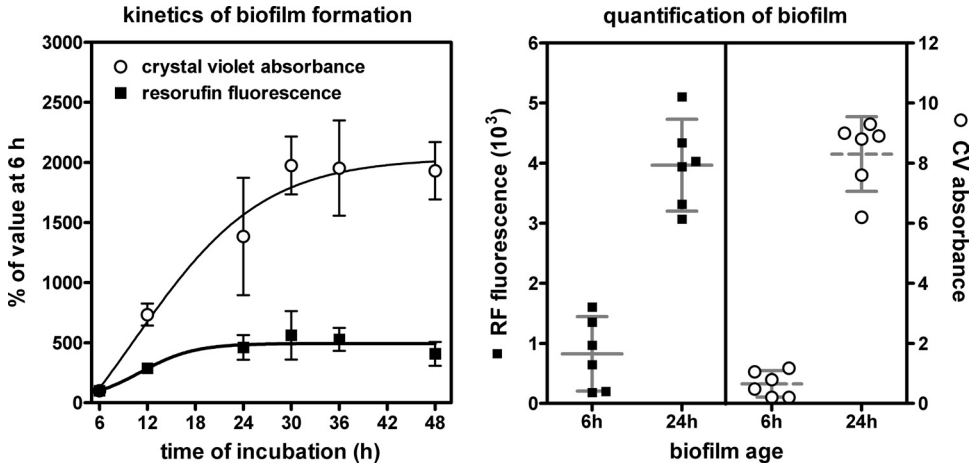

FIG 2 Characterization of the biofilm model with MSSA ATCC 25923. (Left) Evolution over time of the crystal violet absorbance (as a marker of biofilm production) and of resorufin fluorescence (as a marker of bacterial viability) for an initial inoculum with an OD_{620} of 0.005 incubated at 30°C. Data are expressed as percentages of the values measured after 6 h of culture and are the means ± SD of 2 independent experiments, each performed on 8 wells. (Right) Resorufin fluorescence signal (RF; left) and crystal violet absorbance (CV; right) measured for 6-h and 24-h biofilms in 6 independent experiments. Each symbol corresponds to the mean of the results for 8 wells in a single experiment; the horizontal lines and whiskers show the means ± 95% confidence intervals.

RESULTS

Establishing culture conditions for resorufin assay. As a preliminary step in this work, we determined the optimal conditions for assaying bacterial viability using resazurin reduction as a marker. To this effect, we examined the influence of incubation time with resazurin on resorufin fluorescence for planktonic cultures of MSSA ATCC 25923 at increasing OD_{620} values. A linear relationship was observed over a wide range of OD_{620} values for an incubation time of 30 min (Fig. 1, left). For shorter or longer incubation times, the relationship was not linear, which could be interpreted as denoting (i) an inadequate metabolization of resazurin with small inocula after 10 min and (ii) partial exhaustion of the substrate for large inocula when the incubation time was prolonged to 60 min. The relationship between the fluorescence signal after 30 min of incubation and the bacterial load was examined by measuring the OD_{620} of the suspension and counting CFUs. A linear correlation with both parameters was observed in the range of fluorescence signals corresponding to those measured in biofilms in further experiments (Fig. 1, right). Similar data were obtained for the MRSA strain (not shown).

Characterization of the biofilm model. Figure 2 (left) shows the increase with time of crystal violet absorbance (as a marker for biofilm matrix production) and of resorufin fluorescence (as a marker for bacterial viability within the biofilm), with values expressed as the percentage of the signal measured at 6 h (time needed to obtain a tiny but visible biofilm in the wells). The crystal violet signal increased as much as 15- to 20-fold from 6 h to 24 to 30 h, thereafter reaching a plateau value, while the resorufin signal increased 4.5- to 6-fold over the same period of time, with no further increase upon prolonged incubation. On this basis, we selected 6 h and 24 h as the incubation times for studying antibiotic activity on young and mature biofilms, respectively. Figure 2 (right) illustrates that for 6 independent experiments, viability- and matrix-associated signals remained almost within the 95% confidence interval, indicating the repeatability of the model. Similar data were obtained for the MRSA strain (not shown).

Antibiotic intrinsic activity (MICs). Table 1 shows the MICs of the antibiotics studied against MSSA ATCC 25923 and MRSA ATCC 33591. The strains were susceptible to all antibiotics (except to oxacillin for the MRSA). Rifampin, moxifloxacin, and delafloxacin showed the lowest MIC values.

Antibiotic activities against 6-h *S. aureus* biofilms. Figure 3 (see also Fig. S2 in the supplemental material for additional drugs) shows the activities of a series of antistaphylococcal antibiotics against MSSA ATCC 25923 and MRSA ATCC 33591 allowed to form biofilms for 6 h and then exposed to antibiotics for 24 h. All antibiotics displayed concentration-dependent effects on both bacterial viability within the biofilm and biofilm mass. These effects developed in parallel, except for linezolid against the MSSA strain and moxifloxacin against the MRSA strain, which required higher concentrations to act upon biofilm mass. Examination of the corresponding pharmacodynamic parameters (Table 2) reveals that all drugs were able to markedly (>75%) reduce viability (except for oxacillin toward the MRSA strain). This effect was generally obtained at low multiples of their MIC or even at sub-MIC concentrations for fusidic acid, delafloxacin, oxacillin, and rifampin against the MSSA strain and for rifampin against the MRSA strain. Moxifloxacin was much less potent against the

TABLE 1 MICs of antibiotics compared to the corresponding human C_{max}

Antibiotic	Human C_{max} in mg/liter (reference)	MIC (mg/liter) for: MSSA ATCC 25923	MIC (mg/liter) for: MRSA ATCC 33591
Vancomycin	50 (28)	1	1
Fusidic acid	35 (28)	0.25	0.25
Moxifloxacin	4 (28)	0.032	0.032
Delafloxacin	10 (29)	0.004	0.004
Daptomycin	94 (28)	0.5	0.5
Oxacillin	63 (28)	0.125	32–64
Rifampin	18 (28)	0.032	0.032
Linezolid	21 (30)	1	1
Tigecycline	1.5 (28)	0.125	0.5

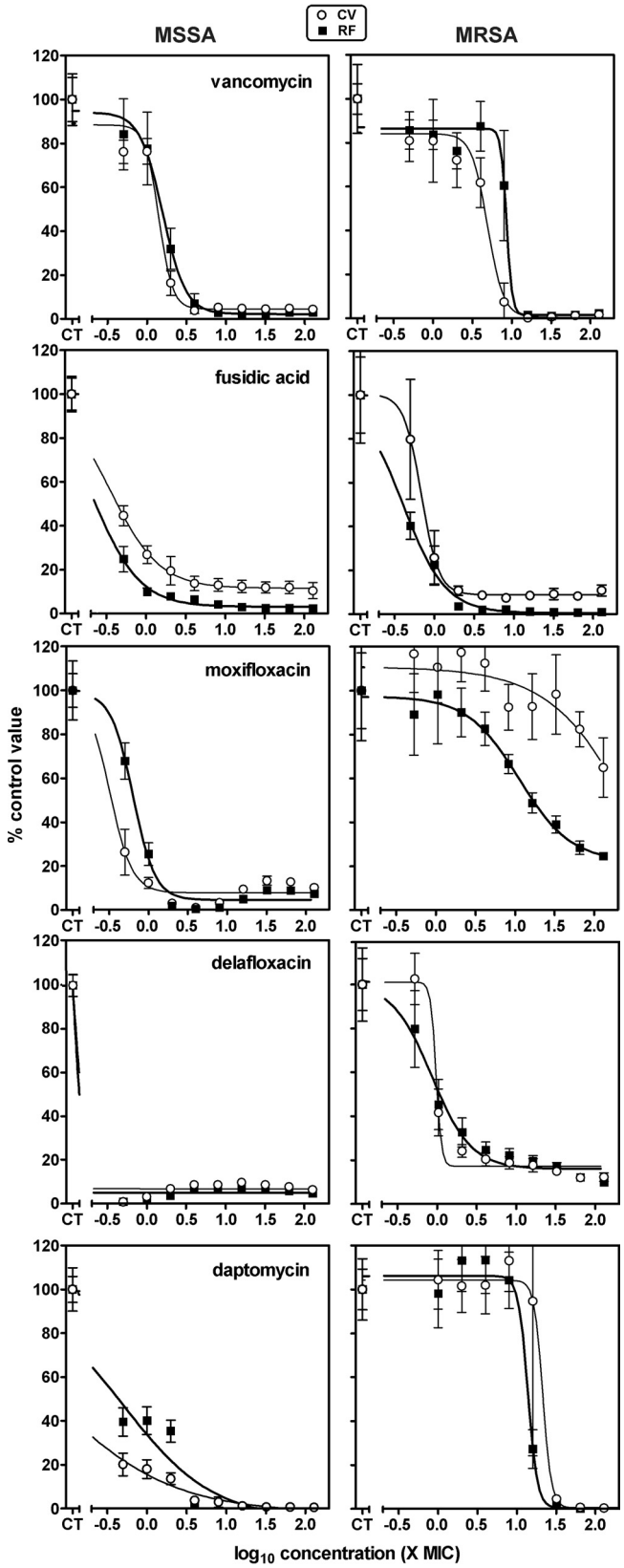

FIG 3 Concentration-response activities of antibiotics against 6-h biofilms of MSSA ATCC 25923 (left) or MRSA ATCC 33591 (right). The 6-h biofilms were incubated with increasing concentrations of antibiotics (shown on the *x* axis) for 24 h. The ordinate shows the change in resorufin fluorescence (RF; filled symbols and thick lines) or in crystal violet absorbance (CV; open symbols and thin lines) as a percentage of the control value (no antibiotic present; CT). All values are the means ± SD of the results for 8 wells (when not visible, the SD bars are smaller than the size of the symbols). The pertinent pharmacological descriptors of the curves are presented in Table 2.

MRSA strain in spite of its low MIC. Considering their effects on the matrix, linezolid was poorly active against the MSSA strain, while moxifloxacin, daptomycin, and oxacillin showed reduced relative potencies against the MRSA strain.

Antibiotic activity against 24-h *S. aureus* biofilms. Figure 4 (see also Figure S3 in the supplemental material for additional antibiotics) and Table 3 show the activities and the corresponding pharmacodynamic parameters for the same antibiotics against 24-h biofilms exposed for 48 h to the drugs under study. Considering effects on viability first, all drugs were much less potent and also less efficacious (except for daptomycin, which remained capable of sterilizing the MSSA biofilm). At clinically achievable concentrations, daptomycin and oxacillin showed the highest efficacies (≥75% effect) against MSSA biofilms, followed by delafloxacin (≥50% effect), fusidic acid, vancomycin, and rifampin (30 to 40%), linezolid and moxifloxacin (≤30%), and tigecycline (~10%). Against MRSA biofilms, all active drugs were more potent than against MSSA, with 50% reduction in viability observed at sub-MIC concentrations for delafloxacin and rifampin at low multiples of the MIC for daptomycin and tigecycline and at still clinically relevant concentrations for moxifloxacin. Vancomycin, fusidic acid, and linezolid achieved lower effects at their human C_{max} (20 to 40% reduction versus the results for the control). The ability of these drugs to reduce biofilm mass was not impressive overall, with only daptomycin and, to some extent, fluoroquinolones being able to act upon the matrix of the MSSA strain and daptomycin, delafloxacin, and rifampin also showing some activity on the MRSA biofilm matrix. In many cases, an increase in the crystal violet signal was observed (values set at 120% in the graphs).

Observation of 24-h *S. aureus* biofilms by confocal microscopy. Biofilms formed on glass coverslips were exposed to selected antibiotics at 32 times their MICs and observed after staining with Live/Dead fluorophores. Figure 5 shows typical 3-dimensional pictures obtained for MSSA and MRSA biofilms, respectively, together with quantitative analyses of the pixels throughout the depth of the biofilm structure. MSSA biofilms were deeper than MRSA biofilms, but viability was similar at equivalent depths. Against both types of biofilms, only delafloxacin and daptomycin significantly decreased bacterial viability at any depth (from ~10% near the surface to ~1% at depths of >10 μm [or even 5 μm for daptomycin against MSSA]). These two drugs were further analyzed at lower multiples of their MICs (Fig. 6; see also the corresponding videos in the supplemental material), with delafloxacin appearing more effective than daptomycin at 8 or 16 times the MIC against the MRSA strain.

DISCUSSION

This study is the first, to our knowledge, to examine in a systematic way the activity of antibiotics (representative of the main antistaphylococcal classes) against *S. aureus* biofilms, considering both biofilm mass and bacterial viability and using complemen-

TABLE 2 Pertinent regression parameters of the dose-response curves[a] for antibiotic activity determined after 24 h of incubation with 6-h biofilm

Antibiotic	Pharmacodynamics[b] determined for indicated strain using:																		
	Resorufin fluorescence									Crystal violet absorbance									
	MSSA					MRSA					MSSA					MRSA				
	E_{max}[d] (% reduction)	Concn (×MIC)[c] yielding specified effect[e]:			Hill slope	E_{max} (% reduction)	Concn (×MIC) yielding specified effect:			Hill slope	E_{max} (% reduction)	Concn (×MIC) yielding specified effect:			Hill slope	E_{max} (% reduction)	Concn (×MIC) yielding specified effect:			Hill slope
		25%	50%	75%			25%	50%	75%			25%	50%	75%			25%	50%	75%	
Vancomycin	97.8	1.0	1.5	2.3	−3.0	98.4	7.4	8.4	9.3	−12.3	95.5	1.0	1.4	2.0	−5	99.5	3.1	4.5	6.1	−4.3
Fusidic acid	97.0	0.1	0.2	0.5	−1.5	99.6	0.2	0.4	0.8	−1.6	88.5	0.2	0.4	1.2	−1.4	91.3	0.5	0.7	1.0	−1.9
Moxifloxacin	95.6	0.5	0.7	1.0	−3.1	78.7	5.5	15.7	103	−1.3	92.3	0.2	0.3	0.5	−3.1	ND	85.6	> 128	> 128	−0.8
Delafloxacin	95.2	< 0.1	< 0.1	< 0.1	−4	84.2	0.5	1.0	2.8	−1.7	93.4	< 0.1	< 0.1	< 0.1	−3.7	83.1	0.9	1.0	1.1	−12.8
Daptomycin	100	0.1	0.4	1.6	−0.8	99.6	12	14	16	−7.1	100	< 0.1	< 0.1	0.4	−0.6	99.5	18	22	25	−7.9
Oxacillin	99.8	< 0.1	< 0.1	0.1	−2.1	ND	> 128	> 128	> 128	NA[f]	99.3	< 0.1	< 0.1	0.1	−2.3	ND	> 128	> 128	> 128	NA
Rifampin	93.5	< 0.1	0.1	0.2	−2.4	92.4	< 0.1	< 0.1	0.1	−0.4	85.2	< 0.1	< 0.1	0.1	−1.7	72.8	< 0.1	< 0.1	> 128	−1.9
Linezolid	88.7	< 0.1	0.3	4.9	−0.5	90.8	0.3	0.6	1.6	−1.3	52.3	1.7	12.8	> 128	−1.6	80.8	0.3	0.6	2.4	−1.4
Tigecycline	92.5	0.9	1.0	1.0	−15	97.8	0.4	0.8	1.9	−1.4	79.3	0.8	1.0	1.8	−4.1	78.9	0.2	0.5	2.3	−1.5

[a] Dose-response curves are illustrated in Figure 3; see also Figure S1 in the supplemental material.

[b] Values were calculated based on sigmoidal regressions (variable slope).

[c] See Table 1 for MIC values.

[d] E_{max} is maximal efficacy, the reduction in signal compared to that of the control for an infinitely large concentration of antibiotics. ND, not determined because the plateau was not reached at the highest concentration tested, preventing us from calculating accurate E_{max} values.

[e] Potency; the concentration needed to reached the specified effect (% reduction from the signal in the control), which is calculated from the equation of the regression for sigmoidal regression ($10^{\{[(\log EC_{50} - \text{Hill slope})/\log[(\text{top} - \text{bottom})/(\text{specified effect} - \text{bottom}) - 1]]/\text{Hill slope}\}}$) (where EC_{50} is 50% effective concentration, top is the Y value at the top plateau, and bottom is the Y value at the bottom plateau) or by graphical intrapolation for biphasic regression.

[f] NA, not applicable (no decrease in signal upon increase in concentration).

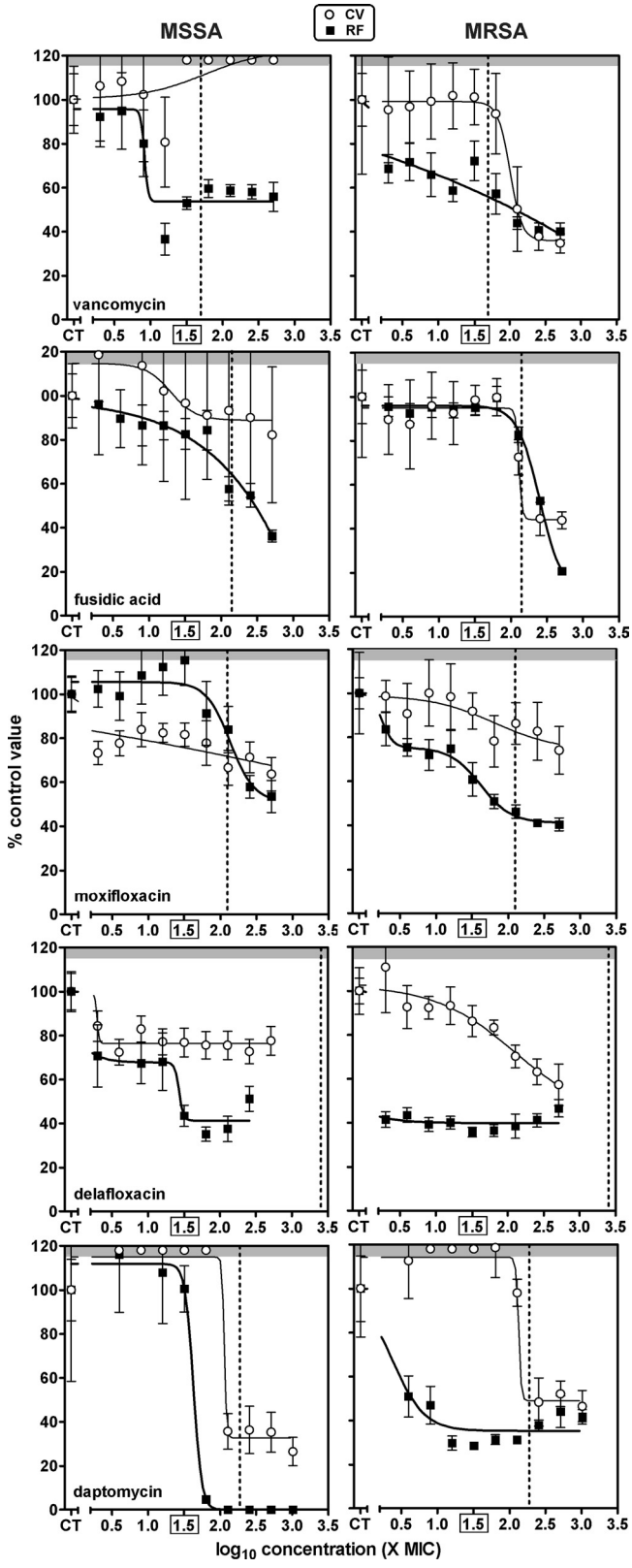

FIG 4 Concentration-response activities of antibiotics against 24-h biofilms of MSSA ATCC 25923 (left) or MRSA ATCC 33591 (right). The 24-h biofilms were incubated with increasing concentrations of antibiotics (shown on the *x* axis) for 48 h. The ordinate shows the change in resorufin fluorescence (RF; filled symbols and thick lines) or in crystal violet absorbance (CV; open symbols and thin lines) as a percentage of the control value (no antibiotic present; CT). Values that are above the control values were set to a value of 120% (highlighted by the gray zone on the graphs). All values are the means ± SD of the results for 8 wells and three independent determinations (when not visible, the SD bars are smaller than the size of the symbols). The pertinent pharmacological descriptors of the curves are presented in Table 3. The vertical dotted lines point to the human C_{max} reached in the serum of patients receiving conventional dosages. The concentrations in boxes correspond to those used for confocal microscopy experiments.

tary quantitative and qualitative approaches. Our methodology has been validated with respect to (i) the reproducibility of the model and (ii) the linearity of the response for the technique used to measure the metabolic activity of bacteria within the biofilm. Specifically, we showed that the time of incubation with resazurin is critical to obtain a linear relationship between the fluorescent signal and the amount of viable bacteria. We also demonstrated that about 6 h of incubation was sufficient to obtain reproducible attachment and matrix production and that 24 h of incubation are sufficient to generate a stable biofilm with *S. aureus*, no major change in the amount of matrix formed being observed upon prolongation of the incubation time. Similar incubation times were also used in many other studies and considered to generate, respectively, a nascent biofilm related to attachment to the support (31–33) and a mature biofilm (6, 15, 34–37). Of note, *in vitro* biofilm formation appears highly dependent on the support (38, 39) and on the medium (40, 41) used, making direct comparisons between models difficult. In particular, we show here that antibiotics seem more active when a biofilm is grown on a glass support (as used for confocal microscopy experiments) than in polypropylene 96-well plates. This is coherent with data in the literature suggesting that *S. aureus* biofilm formation is favored on plastic surfaces (42, 43). Nevertheless, microtiter plate-based models similar to the one used here have demonstrated good correlation with respect to biofilm formation with subcutaneous foreign body infections (38), underlining the potential clinical relevance of the model we developed.

In addition, our data are consistent with previous studies evaluating these methods for quantifying biofilm formation or drug effects (14, 15, 17, 19, 23, 37). However, in contrast to previous studies, our approach allows the characterization of antibiotic activity from a pharmacodynamic perspective. As such, our data provide additional information compared to the minimal biofilm eradication concentration (MBEC) (34), which is the parameter most commonly used to quantify antibiotic effects on biofilms (9, 11, 14, 15, 17, 35, 36).

Considering first our quantitative studies as a whole, all concentration-effect curves follow sigmoid regressions, allowing the comparison of three main pharmacodynamic determinants of antibiotic activity: maximal efficacy, relative potency, and steepness of the dose-response curve. Interestingly enough, antibiotic activity against young biofilms was indistinguishable when considering biofilm mass or viability, with 50% effect reached at reasonably low concentrations compared to the MICs in most cases, suggesting that antibiotic potency is not overly affected in this model.

However, there is a clear influence of biofilm age on antibiotic activity, with loss of efficacy and of potency occurring as the biofilm matures. The 6-h biofilm model represents a situation where bacteria adhere to their support and start producing matrix, while the 24-h model corresponds to a mature biofilm in which matrix

TABLE 3 Pertinent regression parameters of the dose-response curves[a] for antibiotic activity determined after 48 h of incubation with 24-h biofilm

	Pharmacodynamics[b] determined for indicated strain using:																		
	Resorufin fluorescence										Crystal violet absorbance								
	MSSA					MRSA					MSSA					MRSA			
Antibiotic	E_{max}[d] (% reduction)	Concn (×MIC)[c] yielding specified effect[e]: 25%	50%	75%	Hill slope	E_{max} (% reduction)	Concn (×MIC) yielding specified effect: 25%	50%	75%	Hill slope	E_{max} (% reduction)	Concn (×MIC) yielding specified effect: 25%	50%	75%	Hill slope	E_{max} (% reduction)	Concn (×MIC) yielding specified effect: 25%	50%	75%	Hill slope
Vancomycin	46.3	8.2	> 512	> 512	−17	ND	1.6	119	> 512	−0.1	ND	> 512	> 512	> 512	−1.0	64.0	92.0	129	> 512	−5.1
Fusidic acid	76.9	64	296	> 512	−0.5	89.6	168	265	444	−2.8	11.4	> 512	> 512	> 512	−2.5	55.8	126	143	> 512	−19.3
Moxifloxacin	49.0	150.0	> 512	> 512	−2.6	58.2	4.76	66.1	> 512	BP	ND	40.0	> 512	> 512	−0.1	19.7	> 512	> 512	> 512	−1.0
Delafloxacin	64.9	1.3	26.3	> 512	BP[f]	60.2	0.1	0.5	> 512	−1.8	ND	2.3	> 512	> 512	−28.6	58.9	86.4	> 512	> 512	−0.8
Daptomycin	100.0	39	43	50	−7.6	64.7	1.8	4.1	> 512	−2.0	67.3	114	120	> 512	−30	51.0	136	159	> 512	−24
Oxacillin	74.2	1.6	2.2	8.2	−4.1	26.4	0.1	> 512	> 512	NA[g]	13.3	> 512	> 512	> 512	NA	10.5	> 512	> 512	> 512	NA
Rifampin	46.4	0.1	> 512	> 512	−0.2	79.4	< 0.1	0.1	77.5	−9.8	ND	> 512	> 512	> 512	NA	58.6	0.3	> 512	> 512	−0.1
Linezolid	36.9	6.2	> 512	> 512	−1.3	30.7	10.5	> 512	> 512	−2.9	9.1	> 512	> 512	> 512	NA	ND	> 512	> 512	> 512	NA
Tigecycline	41.6	93	> 512	> 512	−0.9	83.8	< 0.1	3.3	> 512	−0.1	9.2	> 512	> 512	> 512	NA	ND	> 512	> 512	> 512	NA

[a] Dose-response curves are illustrated in Figure 4; see also Figure S2 in the supplemental material.

[b] Values were calculated based on sigmoidal regressions (variable slope) or biphasic sigmoidal regressions (for delafloxacin toward MSSA and moxifloxacin toward MRSA).

[c] See Table 1 for MIC values.

[d] E_{max} is maximal efficacy, the reduction in signal compared to that for the control for an infinitely large concentration of antibiotics. ND, not determined because the plateau was not reached at the highest concentration tested, preventing us from calculating accurate E_{max} values.

[e] Potency; the concentration needed to reached the specified effect (% reduction from the signal in the control), which is calculated from the equation of the regression for sigmoidal regression ($10^{\{[(\log EC_{50} - \text{Hill slope})/\log[(\text{top} - \text{bottom})/(\text{specified effect} - \text{bottom}) - 1]]/\text{Hill slope}\}}$) (where EC_{50} is 50% effective concentration, top is the Y value at the top plateau, and bottom is the Y value at the bottom plateau) or by graphical intrapolation for biphasic regression.

[f] BP, biphasic sigmoid regression instead of sigmoid with variable slope.

[g] NA, not applicable (no decrease in signal upon increase in concentration).

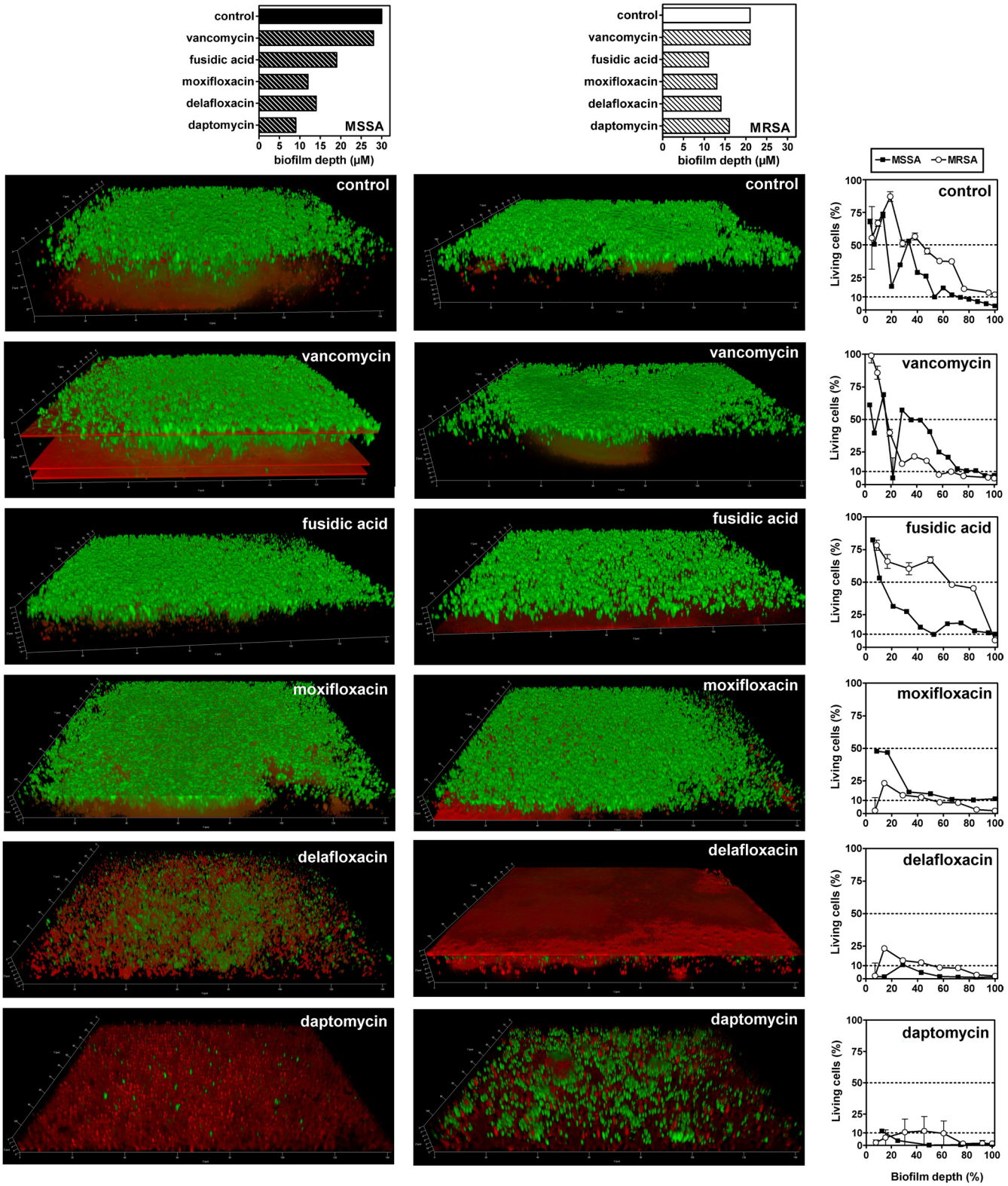

FIG 5 (Left and middle) Three-dimensional images from confocal laser scanning microscopy of 24-h biofilms of MSSA ATCC 25923 (left) and MRSA ATCC 33591 (middle) under control conditions or after exposure to selected antibiotics at 32 times their MICs for 48 h. Biofilms were stained with Syto9 (green; viable cells) and propidium iodide (red; dead cells). All pictures were taken in the same orientation. The depths of the biofilms are shown above. (Right) Quantitative analysis of images, as calculated from the Syto9/propidium iodide fluorescence ratios, presented as the percentages of living cells through the depths of the biofilms (expressed as the percentage of the remaining biofilm under each condition). Statistical analysis was performed using one-way analysis of variance with Dunnett's *post hoc* test versus control: $P < 0.01$ for delafloxacin and daptomycin; $P < 0.05$ for moxifloxacin (MSSA); $P > 0.05$ for vancomycin and fusidic acid (both strains) and moxifloxacin (MRSA).

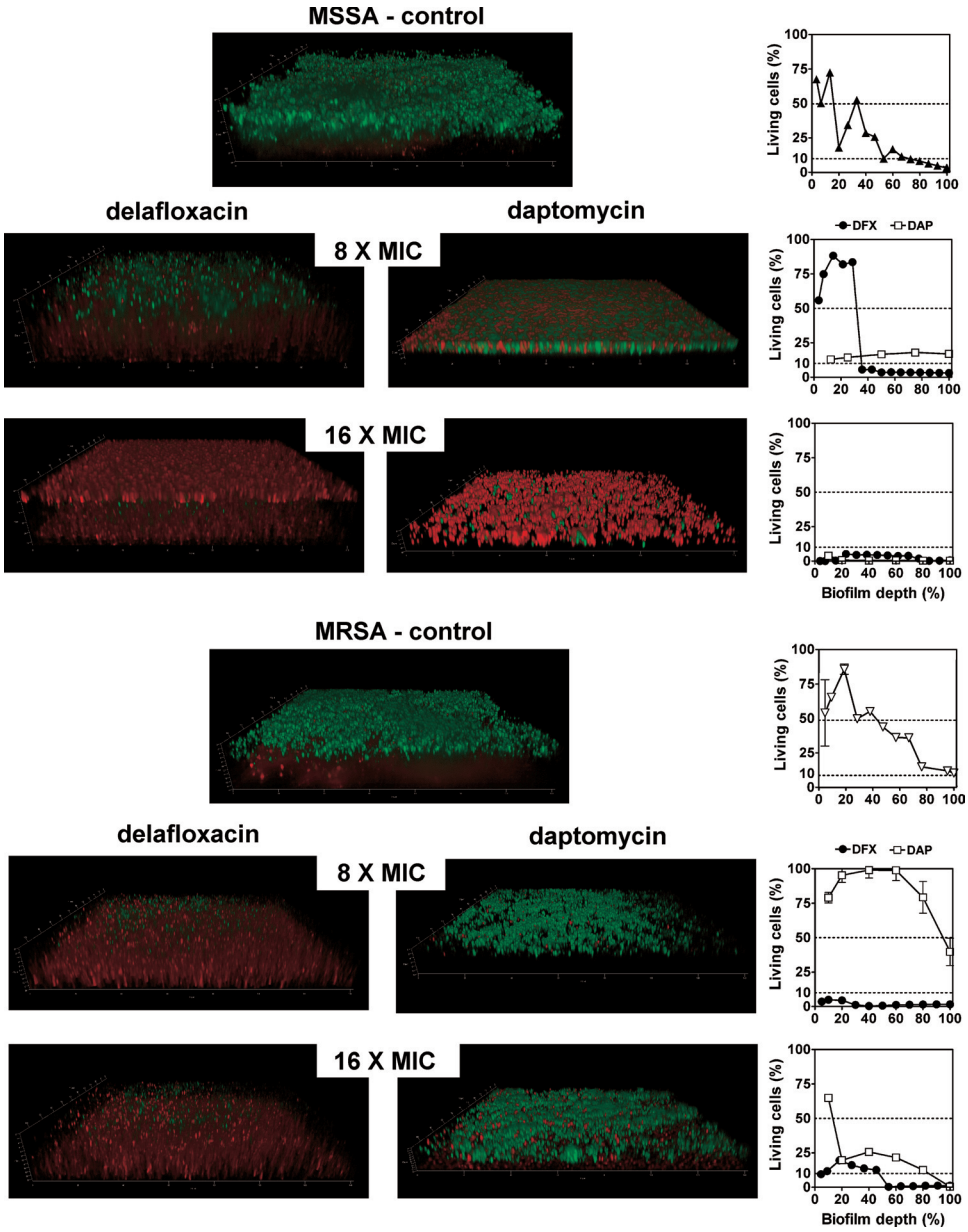

FIG 6 (Left) Three-dimensional images from confocal laser scanning microscopy of 24-h biofilms of MSSA ATCC 25923 (top) or MRSA ATCC 33591 (bottom) under control conditions or after exposure to delafloxacin or daptomycin at 8 and 16 times the respective MIC for 48 h. Biofilms were stained with Syto9 (green; viable cells) and propidium iodide (red; dead cells). Videos showing the 3-dimensional images in various orientations are also available (see the supplemental material). (Right) Percentages of living cells through the depths of the biofilms as calculated from the Syto9/propidium iodide fluorescence ratio (expressed as the percentage of the remaining biofilm under each condition). Statistical analysis was performed using one-way analysis of variance with Tukey *post hoc* test: $P < 0.001$ for delafloxacin (DFX) versus daptomycin (DAP) at 8 times the MIC against MRSA, and for daptomycin, at 8 times the MIC versus 16 times the MIC against MRSA.

production has reached a maximum. We see that the reduction in antibiotic activity with biofilm maturation seems more important with respect to biofilm mass than to bacterial viability. This is consistent with the fact that antibacterial agents act on essential bacterial targets and not upon biofilm matrix. Reductions in biofilm mass are thus likely consecutive to bacterial growth inhibition or killing during the 48 h of exposure to antibiotics, as previously demonstrated for daptomycin or fluoroquinolones (12, 13). Indeed, the antibiotics showing activity in our model also decrease biofilm depth (as observed by confocal microscopy). In contrast, an increase in biofilm mass is observed in many cases where antibiotics had minimal effects on viability and were poorly active. This has been previously observed by others (44–46), essentially upon exposure to low concentrations, and is suggested to result from an induction of a stress response or of the expression of virulence genes (46, 47). It is also interesting to note that antibiotic effects on viability are best seen at the surface of the biofilm or in the deepest zones, which may correspond, respectively, to the regions that are the most accessible to antibiotics (48) or to those where bacterial viability is already compromised, as suggested by

control images. A recent study suggests, however, that lack of activity against biofilms is due not to insufficient diffusion but, rather, to poor bioavailability, with the drug possibly interacting with matrix constituents (49), which are supposedly more abundant where bacteria are metabolically active.

Compared to what was observed previously in experiments of similar design performed against extracellular or intracellular *S. aureus* (50), the steepness of the dose-response curve (Hill slope) is in several cases much higher than −1 (more-negative values), suggesting that response to the drugs can be amplified as soon as biofilm starts to be damaged. Also noteworthy, the concentration-effect relationships at 24 h for fluoroquinolones were fitted best using double sigmoid curves when considering the effect of delafloxacin against the MSSA strain and that of moxifloxacin against the MRSA strain. Although the reason for this specific behavior is still unknown, it was previously observed when examining the intracellular activity of delafloxacin against the same MSSA strain (51) and attributed to its dual targeting of DNA gyrase and topoisomerase IV.

Beside biofilm maturity, the bacterial strain also clearly influences antibiotic activity. In spite of the fact that the control signals for viability and biofilm mass were similar for the two strains investigated and that the MICs for most antibiotics were similar against both strains, we see that antibiotic activity, at equipotent concentrations, is usually higher against the MRSA strain. Although we currently have no simple explanation for this observation with these particular strains, this may well reflect differences in the nature and/or the biophysical properties of the biofilm produced, ultimately affecting antibiotic bioavailability and/or expression of activity. The mechanisms of biofilm formation indeed depend on different regulatory pathways in MSSA and MRSA (52, 53), with specific determinants like the *agr* group, polysaccharide intercellular adhesin production, and *spa* types being more determinant for the capacity to produce slime than the expression of microbial surface components recognizing adhesive matrix molecules (MSCRAMM) (4, 54, 55). The nature of the biofilm matrix can differ among strains as well, with some producing a polysaccharide-based matrix under the control of the *ica* locus and others producing a protein-based matrix (4). A strong correlation has been observed between *ica* operon transcription and polysaccharide production in MSSA strains but not in MRSA strains (56).

Examining, then, antibiotic activity from a clinical perspective, we show that most of the current antistaphylococcal agents are poorly effective and weakly potent against mature biofilms, possibly rationalizing therapeutic failures (57). The drugs that prove the most effective to kill bacteria in this model are fusidic acid, fluoroquinolones, and daptomycin, while the most potent are delafloxacin and daptomycin, making the two latter molecules potentially useful therapeutic options. Daptomycin activity against biofilms has been documented in several *in vitro* and *in vivo* models (6, 8–10, 12, 16). It is globally considered more active than fluoroquinolones (6, 9) (in particular, moxifloxacin [8, 13]), despite the fact that both drugs show similar MICs and are highly bactericidal against planktonic bacteria. Accordingly, daptomycin has been considered for the treatment of infections possibly involving biofilms, such as catheter-related bloodstream infections (58), right-side endocarditis (59, 60), or cardiac implantable electronic device-related infective endocarditis (61). Interestingly, we show here that delafloxacin is also clearly more effective than moxifloxacin at equipotent concentrations, suggesting that factors other than higher intrinsic activity (low MIC value) play a role in this context. A possible explanation could reside in a local environment favorable to the expression of delafloxacin activity within the biofilm. We know, for example, that delafloxacin, in contrast to daptomycin, gains potency in acidic environments (51), which may be the case within biofilms, as suggested from studies on biofilms of *Pseudomonas* or streptococci (62, 63). Delafloxacin even seems to be more active than daptomycin against the MRSA strain at equipotent concentrations, suggesting that further comparisons of the activities of these two drugs against biofilms from recent clinical isolates should be conducted.

Thus, taken together, the experimental approach proposed here has generated a comprehensive analysis of the pharmacodynamic parameters defining antibiotic activity against biofilms of *S. aureus*. It has highlighted the importance of the maturity of the biofilm and of the strain involved as determinants of antibiotic activity, suggesting the importance of better defining biofilm biophysical or chemical properties influencing antibiotic action. Thus, the apparent resistance to antibiotics of bacteria growing in biofilms is probably multifactorial, with a combination of mechanisms that are both innate (decreases in antibiotic access, oxygen, and nutrient availability and lower metabolic activity) or induced by antibiotic exposure (like stress response and/or a switch to a persister phenotype) (64, 65). From a clinical point of view, this study has also allowed the ranking of antistaphylococcal agents in regard to their respective interest for treating biofilm-related infections, paving the way for the design of pertinent *in vivo* or clinical studies.

ACKNOWLEDGMENTS

K. Santos and S. Wongpramud provided dedicated technical assistance. We thank the manufacturers for providing us with free samples of their antibiotics.

Conflict of interest: P.M.T. and F.V.B. have received a research grant from Rib-X Pharmaceuticals.

This work was supported by the Belgian Fonds pour la Recherche Scientifique Médicale (grant 3.4530.12), research programs from the Region bruxelloise (Innoviris), and a grant-in-aid from Rib-X Pharmaceuticals. J.B. was a postdoctoral fellow of the program Brains Back to Brussels, and W.S. is a postdoctoral fellow of the program Prospective Research for Brussels of the Région Bruxelloise, Belgium. F.V.B. is Maître de Recherches of the Belgian Fonds National de la Recherche Scientifique.

REFERENCES

1. **Archer NK, Mazaitis MJ, Costerton JW, Leid JG, Powers ME, Shirtliff ME.** 2011. Staphylococcus aureus biofilms: properties, regulation, and roles in human disease. Virulence **2**:445–459.
2. **Hall-Stoodley L, Stoodley P.** 2009. Evolving concepts in biofilm infections. Cell. Microbiol. **11**:1034–1043.
3. **Barretti P, Moraes TM, Camargo CH, Caramori JC, Mondelli AL, Montelli AC, da Cunha ML.** 2012. Peritoneal dialysis-related peritonitis due to Staphylococcus aureus: a single-center experience over 15 years. PLoS One **7**:e31780. doi:10.1371/journal.pone.0031780.
4. **Speziale P, Visai L, Rindi S, Pietrocola G, Provenza G, Provenzano M.** 2008. Prevention and treatment of Staphylococcus biofilms. Curr. Med. Chem. **15**:3185–3195.
5. **Otto M.** 2008. Staphylococcal biofilms. Curr. Top. Microbiol. Immunol. **322**:207–228.
6. **Kirby AE, Garner K, Levin BR.** 2012. The relative contributions of physical structure and cell density to the antibiotic susceptibility of bacteria in biofilms. Antimicrob. Agents Chemother. **56**:2967–2975.
7. **Raad I, Hanna H, Jiang Y, Dvorak T, Reitzel R, Chaiban G, Sherertz R, Hachem R.** 2007. Comparative activities of daptomycin, linezolid, and tigecycline against catheter-related methicillin-resistant Staphylococcus

bacteremic isolates embedded in biofilm. Antimicrob. Agents Chemother. **51**:1656–1660.
8. **Parra-Ruiz J, Vidaillac C, Rose WE, Rybak MJ.** 2010. Activities of high-dose daptomycin, vancomycin, and moxifloxacin alone or in combination with clarithromycin or rifampin in a novel in vitro model of Staphylococcus aureus biofilm. Antimicrob. Agents Chemother. **54**: 4329–4334.
9. **Cafiso V, Bertuccio T, Spina D, Purrello S, Stefani S.** 2010. Tigecycline inhibition of a mature biofilm in clinical isolates of Staphylococcus aureus: comparison with other drugs. FEMS Immunol. Med. Microbiol. **59**:466–469.
10. **LaPlante KL, Woodmansee S.** 2009. Activities of daptomycin and vancomycin alone and in combination with rifampin and gentamicin against biofilm-forming methicillin-resistant Staphylococcus aureus isolates in an experimental model of endocarditis. Antimicrob. Agents Chemother. **53**:3880–3886.
11. **LaPlante KL, Mermel LA.** 2009. In vitro activities of telavancin and vancomycin against biofilm-producing Staphylococcus aureus, S. epidermidis, and Enterococcus faecalis strains. Antimicrob. Agents Chemother. **53**:3166–3169.
12. **Roveta S, Marchese A, Schito GC.** 2008. Activity of daptomycin on biofilms produced on a plastic support by Staphylococcus spp. Int. J. Antimicrob. Agents **31**:321–328.
13. **Roveta S, Schito AM, Marchese A, Schito GC.** 2007. Activity of moxifloxacin on biofilms produced in vitro by bacterial pathogens involved in acute exacerbations of chronic bronchitis. Int. J. Antimicrob. Agents **30**: 415–421.
14. **Reiter KC, Sambrano GE, Villa B, Paim TG, de Oliveira CF, d'Azevedo PA.** 2012. Rifampicin fails to eradicate mature biofilm formed by methicillin-resistant Staphylococcus aureus. Rev. Soc. Bras. Med. Trop. **45**:471–474.
15. **Wu WS, Chen CC, Chuang YC, Su BA, Chiu YH, Hsu HJ, Ko WC, Tang HJ.** 9 May 2012. Efficacy of combination oral antimicrobial agents against biofilm-embedded methicillin-resistant Staphylococcus aureus. J. Microbiol. Immunol. Infect. [Epub ahead of print.] doi:10.1016/j.jmii.2012.03.009.
16. **Smith K, Perez A, Ramage G, Gemmell CG, Lang S.** 2009. Comparison of biofilm-associated cell survival following in vitro exposure of meticillin-resistant Staphylococcus aureus biofilms to the antibiotics clindamycin, daptomycin, linezolid, tigecycline and vancomycin. Int. J. Antimicrob. Agents **33**:374–378.
17. **Cha JO, Park YK, Lee YS, Chung GT.** 2011. In vitro biofilm formation and bactericidal activities of methicillin-resistant Staphylococcus aureus clones prevalent in Korea. Diagn. Microbiol. Infect. Dis. **70**:112–118.
18. **Tote K, Berghe DV, Deschacht M, de Wit K, Maes L, Cos P.** 2009. Inhibitory efficacy of various antibiotics on matrix and viable mass of Staphylococcus aureus and Pseudomonas aeruginosa biofilms. Int. J. Antimicrob. Agents **33**:525–531.
19. **Sandberg ME, Schellmann D, Brunhofer G, Erker T, Busygin I, Leino R, Vuorela PM, Fallarero A.** 2009. Pros and cons of using resazurin staining for quantification of viable Staphylococcus aureus biofilms in a screening assay. J. Microbiol. Methods **78**:104–106.
20. **Hostacka A, Ciznar I, Stefkovicova M.** 2010. Temperature and pH affect the production of bacterial biofilm. Folia Microbiol. (Praha) **55**:75–78.
21. **Pagedar A, Singh J, Batish VK.** 2010. Surface hydrophobicity, nutritional contents affect Staphylococcus aureus biofilms and temperature influences its survival in preformed biofilms. J. Basic Microbiol. **50**(Suppl 1): S98–S106.
22. **Christensen GD, Simpson WA, Bisno AL, Beachey EH.** 1982. Adherence of slime-producing strains of Staphylococcus epidermidis to smooth surfaces. Infect. Immun. **37**:318–326.
23. **Tote K, Horemans T, Vanden Berghe D, Maes L, Cos P.** 2010. Inhibitory effect of biocides on the viable masses and matrices of Staphylococcus aureus and Pseudomonas aeruginosa biofilms. Appl. Environ. Microbiol. **76**:3135–3142.
24. **Tote K, Vanden Berghe D, Maes L, Cos P.** 2008. A new colorimetric microtitre model for the detection of Staphylococcus aureus biofilms. Lett. Appl. Microbiol. **46**:249–254.
25. **Clinical and Laboratory Standards Institute.** 2012. Performance standards for antimicrobial susceptibility testing, 22nd informational supplement. CLSI document MS100-S22. Clinical and Laboratory Standards Institute, Wayne, PA.
26. **Maukonen J, Alakomi HL, Nohynek K, Hallamaa S, Leppämäki S, Mättö J, Saarela M.** 2006. Suitability of the fluorescent techniques for the enumeration of probiotic bacteria in commercial non-dairy drinks and pharmaceutical products. Food Res. Int. **39**:22–32.
27. **Fernandez-Barat L, Li BG, Ferrer M, Bosch A, Calvo M, Vila J, Gabarrus A, Martinez-Olondris P, Rigol M, Esperatti M, Luque N, Torres A.** 2012. Direct analysis of bacterial viability in endotracheal tube biofilm from a pig model of methicillin-resistant Staphylococcus aureus pneumonia following antimicrobial therapy. FEMS Immunol. Med. Microbiol. **65**:309–317.
28. **Amsden GW.** 2009. Tables of antimicrobial agent pharmacology, p 705–764. *In* Mandell GL, Bennett JE, Dolin R (ed), Mandell, Douglas, and Bennett's principles and practice of infectious diseases, 7th ed. Elsevier, Philadelphia, PA.
29. **Lawrence L, Benedict M, Hart J, Hawkins A, Li D, Medlock M, Hopkins S, Burak E.** 2011. Pharmacokinetics (PK) and safety of single doses of delafloxacin administered intravenously in healthy human subjects, poster A2-045a. Abstr. 51st Intersci. Conf. Antimicrob. Agents Chemother. (ICAAC). American Society for Microbiology, Washington, DC.
30. **Anonymous.** 2005. Zyvox. U.S. full prescribing information. Pharmacia & Upjohn, Division of Pfizer, Inc., New York, NY.
31. **Gracia E, Fernandez A, Conchello P, Lacleriga A, Paniagua L, Seral F, Amorena B.** 1997. Adherence of Staphylococcus aureus slime-producing strain variants to biomaterials used in orthopaedic surgery. Int. Orthop. **21**:46–51.
32. **Saldarriaga Fernández IC, Mei IHC, Metzger S, Grainger DW, Engelsman AF, Nejadnik MR, Busscher HJ.** 2010. In vitro and in vivo comparisons of staphylococcal biofilm formation on a cross-linked poly(ethylene glycol)-based polymer coating. Acta Biomater. **6**:1119–1124.
33. **Amorena B, Gracia E, Monzon M, Leiva J, Oteiza C, Perez M, Alabart JL, Hernandez-Yago J.** 1999. Antibiotic susceptibility assay for Staphylococcus aureus in biofilms developed in vitro. J. Antimicrob. Chemother. **44**:43–55.
34. **Ceri H, Olson ME, Stremick C, Read RR, Morck D, Buret A.** 1999. The Calgary Biofilm Device: new technology for rapid determination of antibiotic susceptibilities of bacterial biofilms. J. Clin. Microbiol. **37**:1771–1776.
35. **Mataraci E, Dosler S.** 2012. In vitro activities of antibiotics and antimicrobial cationic peptides alone and in combination against methicillin-resistant Staphylococcus aureus biofilms. Antimicrob. Agents Chemother. **56**:6366–6371.
36. **Reiter KC, Villa B, Silva Paim TG, Sambrano GE, de Oliveira CF, d'Azevedo PA.** 2012. Enhancement of antistaphylococcal activities of six antimicrobials against sasG-negative methicillin-susceptible Staphylococcus aureus: an in vitro biofilm model. Diagn. Microbiol. Infect. Dis. **74**: 101–105.
37. **Skogman ME, Vuorela PM, Fallarero A.** 2012. Combining biofilm matrix measurements with biomass and viability assays in susceptibility assessments of antimicrobials against Staphylococcus aureus biofilms. J. Antibiot. (Tokyo). **65**:453–459.
38. **Ferreira FA, Souza RR, Bonelli RR, Americo MA, Fracalanzza SE, Figueiredo AM.** 2012. Comparison of in vitro and in vivo systems to study ica-independent Staphylococcus aureus biofilms. J. Microbiol. Methods **88**:393–398.
39. **Wagner C, Aytac S, Hansch GM.** 2011. Biofilm growth on implants: bacteria prefer plasma coats. Int. J. Artif. Organs **34**:811–817.
40. **Cassat JE, Lee CY, Smeltzer MS.** 2007. Investigation of biofilm formation in clinical isolates of Staphylococcus aureus. Methods Mol. Biol. **391**:127–144.
41. **Fitzpatrick F, Humphreys H, O'Gara JP.** 2006. Environmental regulation of biofilm development in methicillin-resistant and methicillin-susceptible Staphylococcus aureus clinical isolates. J. Hosp. Infect. **62**: 120–122.
42. **Gross M, Cramton SE, Gotz F, Peschel A.** 2001. Key role of teichoic acid net charge in Staphylococcus aureus colonization of artificial surfaces. Infect. Immun. **69**:3423–3426.
43. **Lim Y, Jana M, Luong TT, Lee CY.** 2004. Control of glucose- and NaCl-induced biofilm formation by rbf in Staphylococcus aureus. J. Bacteriol. **186**:722–729.
44. **Kaplan JB, Izano EA, Gopal P, Karwacki MT, Kim S, Bose JL, Bayles KW, Horswill AR.** 2012. Low levels of beta-lactam antibiotics induce extracellular DNA release and biofilm formation in Staphylococcus aureus. mBio **3**(4):e00198–12. doi:10.1128/mBio.00198-12.
45. **Mirani ZA, Jamil N.** 2011. Effect of sub-lethal doses of vancomycin and

oxacillin on biofilm formation by vancomycin intermediate resistant Staphylococcus aureus. J. Basic Microbiol. **51**:191–195.
46. **Subrt N, Mesak LR, Davies J.** 2011. Modulation of virulence gene expression by cell wall active antibiotics in Staphylococcus aureus. J. Antimicrob. Chemother. **66**:979–984.
47. **Kaplan JB.** 2011. Antibiotic-induced biofilm formation. Int. J. Artif. Organs **34**:737–751.
48. **Singh R, Ray P, Das A, Sharma M.** 2010. Penetration of antibiotics through Staphylococcus aureus and Staphylococcus epidermidis biofilms. J. Antimicrob. Chemother. **65**:1955–1958.
49. **Daddi Oubekka S, Briandet R, Fontaine-Aupart MP, Steenkeste K.** 2012. Correlative time-resolved fluorescence microscopy to assess antibiotic diffusion-reaction in biofilms. Antimicrob. Agents Chemother. **56**: 3349–3358.
50. **Barcia-Macay M, Seral C, Mingeot-Leclercq MP, Tulkens PM, Van Bambeke F.** 2006. Pharmacodynamic evaluation of the intracellular activities of antibiotics against Staphylococcus aureus in a model of THP-1 macrophages. Antimicrob. Agents Chemother. **50**:841–851.
51. **Lemaire S, Tulkens PM, Van Bambeke F.** 2011. Contrasting effects of acidic pH on the extracellular and intracellular activities of the anti-gram-positive fluoroquinolones moxifloxacin and delafloxacin against Staphylococcus aureus. Antimicrob. Agents Chemother. **55**:649–658.
52. **Pozzi C, Waters EM, Rudkin JK, Schaeffer CR, Lohan AJ, Tong P, Loftus BJ, Pier GB, Fey PD, Massey RC, O'Gara JP.** 2012. Methicillin resistance alters the biofilm phenotype and attenuates virulence in Staphylococcus aureus device-associated infections. PLoS Pathog. **8**:e1002626. doi:10.1371/journal.ppat.1002626.
53. **Liesse Iyamba JM, Seil M, Devleeschouwer M, Takaisi Kikuni NB, Dehaye JP.** 2011. Study of the formation of a biofilm by clinical strains of Staphylococcus aureus. Biofouling **27**:811–821.
54. **Atshan SS, Nor SM, Sekawi Z, Lung LT, Hamat RA, Karunanidhi A, Mateg AA, Ghaznavi-Rad E, Ghasemzadeh-Moghaddam H, Chong Seng JS, Nathan JJ, Pei PC.** 2012. Prevalence of adhesion and regulation of biofilm-related genes in different clones of Staphylococcus aureus. J. Biomed. Biotechnol. **2012**:976972. doi:10.1155/2012/976972.
55. **Ikonomidis A, Vasdeki A, Kristo I, Maniatis AN, Tsakris A, Malizos KN, Pournaras S.** 2009. Association of biofilm formation and methicillin-resistance with accessory gene regulator (agr) loci in Greek Staphylococcus aureus clones. Microb. Pathog. **47**:341–344.
56. **O'Neill E, Pozzi C, Houston P, Smyth D, Humphreys H, Robinson DA, O'Gara JP.** 2007. Association between methicillin susceptibility and biofilm regulation in Staphylococcus aureus isolates from device-related infections. J. Clin. Microbiol. **45**:1379–1388.
57. **Falagas ME, Kapaskelis AM, Kouranos VD, Kakisi OK, Athanassa Z, Karageorgopoulos DE.** 2009. Outcome of antimicrobial therapy in documented biofilm-associated infections: a review of the available clinical evidence. Drugs **69**:1351–1361.
58. **Chaftari AM, Hachem R, Mulanovich V, Chemaly RF, Adachi J, Jacobson K, Jiang Y, Raad I.** 2010. Efficacy and safety of daptomycin in the treatment of Gram-positive catheter-related bloodstream infections in cancer patients. Int. J. Antimicrob. Agents **36**:182–186.
59. **Das I, Saluja T, Steeds R.** 2011. Use of daptomycin in complicated cases of infective endocarditis. Eur. J. Clin. Microbiol. Infect. Dis. **30**:807–812.
60. **Segreti JA, Crank CW, Finney MS.** 2006. Daptomycin for the treatment of gram-positive bacteremia and infective endocarditis: a retrospective case series of 31 patients. Pharmacotherapy **26**:347–352.
61. **Durante-Mangoni E, Casillo R, Bernardo M, Caianiello C, Mattucci I, Pinto D, Agrusta F, Caprioli R, Albisinni R, Ragone E, Utili R.** 2012. High-dose daptomycin for cardiac implantable electronic device-related infective endocarditis. Clin. Infect. Dis. **54**:347–354.
62. **Hunter RC, Beveridge TJ.** 2005. Application of a pH-sensitive fluoroprobe (C-SNARF-4) for pH microenvironment analysis in Pseudomonas aeruginosa biofilms. Appl. Environ. Microbiol. **71**:2501–2510.
63. **Schlafer S, Raarup MK, Meyer RL, Sutherland DS, Dige I, Nyengaard JR, Nyvad B.** 2011. pH landscapes in a novel five-species model of early dental biofilm. PLoS One **6**:e25299. doi:10.1371/journal.pone.0025299.
64. **Anderson GG, O'Toole GA.** 2008. Innate and induced resistance mechanisms of bacterial biofilms. Curr. Top. Microbiol. Immunol. **322**:85–105.
65. **Mah TF, O'Toole GA.** 2001. Mechanisms of biofilm resistance to antimicrobial agents. Trends Microbiol. **9**:34–39.

A combined pharmacodynamic quantitative and qualitative model reveals the potent activity of Daptomycin and Delafloxacin against S*taphylococcus aureus* biofilms

Julia Bauer,[$,#] Wafi Siala,[#] Paul M. Tulkens, and Françoise Van Bambeke

Pharmacologie cellulaire et moléculaire, Louvain Drug Research Institute, Université catholique de Louvain, Brussels, Belgium

Supplemental material

Figure S1

Relationship between the green/red fluorescence ratio of LIVE/DEAD staining of bacterial suspensions as observed in confocal laser scanning microscopy (CLSM; upper panel) and the percentage of live bacteria in the suspension (0-10-50-90-100 % in the upper panel pictures).

Samples were prepared by adding 500µl of Tryptic Soy Broth supplemented with 0.25% glucose and 0.5% NaCl to an established biofilm, which was immediately sonicated (2 times during 15 s; Branson 3510 ultrasonic cleaner). The bacterial suspension was then placed in a sterile tube, centrifuged (10min, 10000g), washed and resuspended in 250µl phosphate buffered saline (PBS; live cells) or PBS containing 10mg/ml cetrimide (dead cells), and incubated for 2h at room temperature with shaking. Live and dead cells were mixed at different ratios in a final volume of 100µl. Samples were centrifuged (10min, 10000g) and pellets incubated during 30 min at room temperature in the dark with 200 µl of LIVE/DEAD staining solution. Samples were centrifuged again, resuspended with 20µl of LIVE/DEAD staining solution and observed in CLSM. The fluorescence emission ratio of each sample was then calculated to establish a titration curve in function of the percentage of live/dead cells in the sample (slope: 0.082; Y intercept: 0.214; R^2: 0.994).

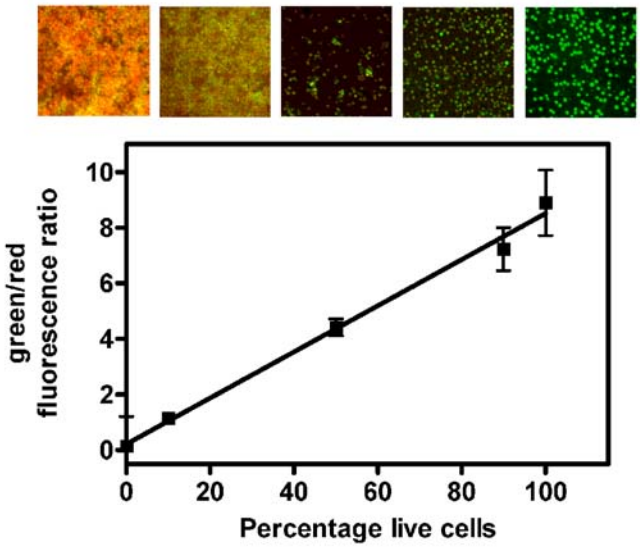

Figure S2

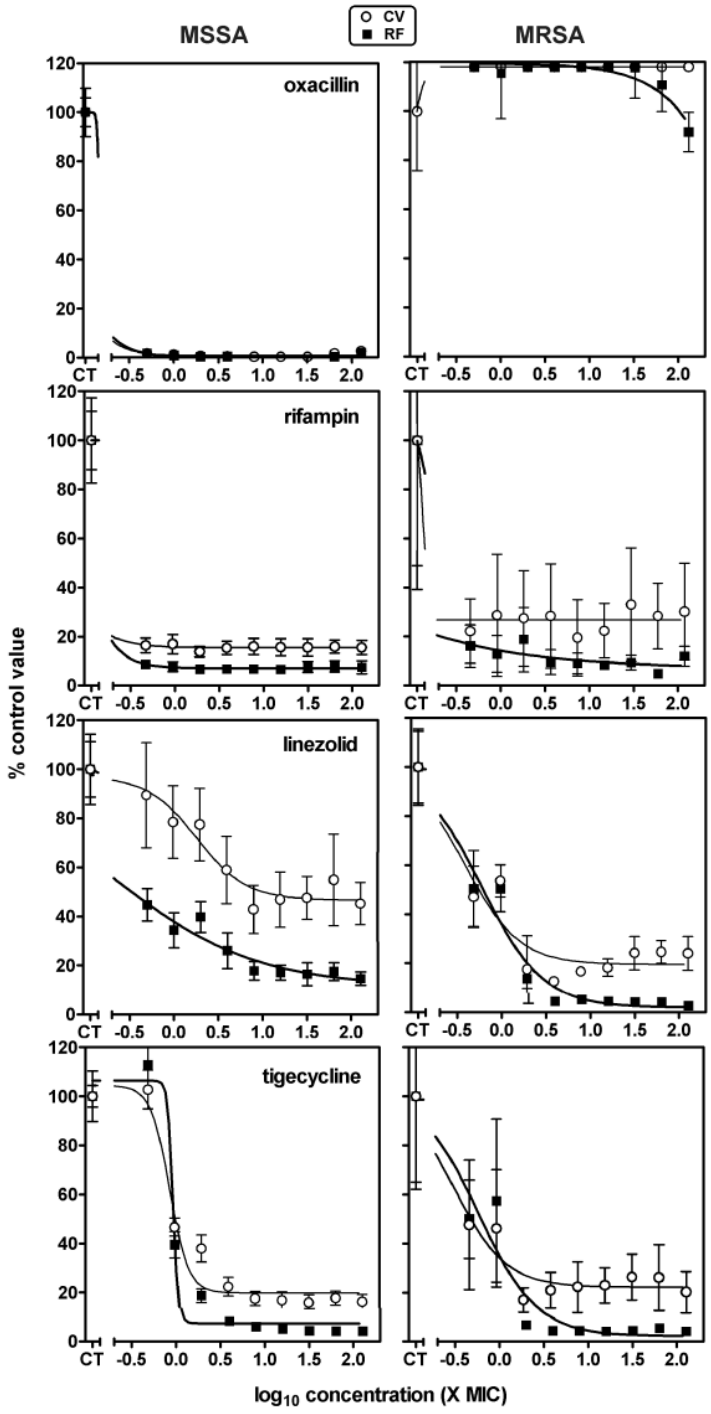

Concentration-response activity of antibiotics against 6h biofilms of MSSA ATCC25923 (left) or MRSA ATCC33591 (right). 6-h biofilms were incubated with increasing concentrations of antibiotics for 24 h. The ordinate shows the change in resorufin fluorescence (filled symbols and thick lines) or in crystal violet absorbance (open symbols and thin lines) in percentage of the control value (no antibiotic present). All values are means ± standard deviations (SD) of 8 wells (when not visible, the SD bars are smaller than the size of the symbols). The pertinent pharmacological descriptors of the curves are presented in Table 2.

Figure S3

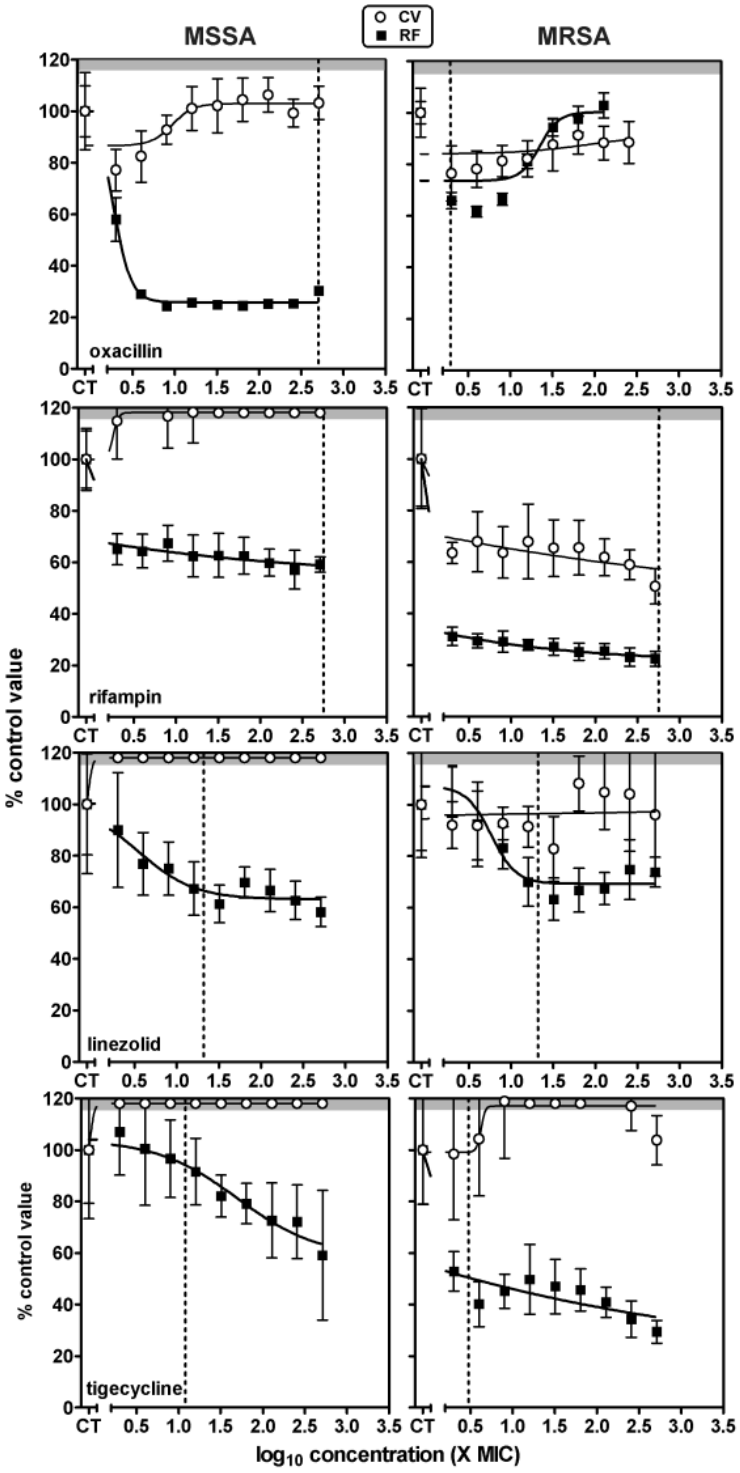

Concentration-response activity of antibiotics against 24-h biofilms of MSSA ATCC25923 (left) or MRSA ATCC33591 (right). 24-h biofilms were incubated with increasing concentrations of antibiotics for 48 h. The ordinate shows the change in resorufin fluorescence (filled symbols and thick lines) or in crystal violet absorbance (open symbols and thin lines) in percentage of the control value (no antibiotic present). Values that are above controls have been set to a value of 120 % (highlighted by the grey zone on the graphs). All values are means ± standard deviations (SD) of 8 wells three independent determinations (when not visible, the SD bars are smaller than the size of the symbols). The pertinent pharmacological descriptors of the curves are presented in Table 3. The vertical dotted lines point to the human C_{max} reached in the serum of patients receiving conventional dosages.